Lennart Volz*, Charles-Antoine Collins-Fekete, Pierluigi Piersimoni, Robert P. Johnson, Vladimir Bashkirov, Reinhard Schulte and Joao Seco

Stopping power accuracy and achievable spatial resolution of helium ion imaging using a prototype particle CT detector system

Abstract: A precise relative stopping power map of the patient is crucial for accurate particle therapy. Charged particle imaging determines the stopping power either tomographically – particle computed tomography (pCT) – or by combining prior knowledge from particle radiography (pRad) and x-ray CT. Generally, multiple Coulomb scattering limits the spatial resolution. Compared to protons, heavier particles scatter less due to their lower charge/mass ratio. A theoretical framework to predict the most likely trajectory of particles in matter was developed for light ions up to carbon and was found to be the most accurate for helium comparing for fixed initial velocity. To further investigate the potential of helium in particle imaging, helium computed tomography (HeCT) and radiography (HeRad) were studied at the Heidelberg Ion-Beam Therapy Centre (HIT) using a prototype pCT detector system registering individual particles, originally developed by the U.S. pCT collaboration. Several phantoms were investigated: modules of the Catphan QA phantom for analysis of spatial resolution and achievable stopping power accuracy, a paediatric head phantom (CIRS) and a custom-made phantom comprised of animal meat enclosed in a 2 % agarose mixture representing human tissue. The pCT images were reconstructed applying the CARP iterative reconstruction algorithm. The $MTF_{10\%}$ was investigated using a sharp edge gradient technique. HeRad provides a spatial resolution above that of protons ($MTF10_{10\%}$=6.07 lp/cm for HeRad versus $MTF_{10\%}$=3.35 lp/cm for proton radiography). For HeCT, the spatial resolution was limited by the number of projections acquired (90 projections for a full scan). The RSP accuracy for all inserts of the Catphan CTP404 module was found to be 2.5% or better and is subject to further optimisation. In conclusion, helium imaging appears to offer higher spatial resolution compared to proton imaging. In future studies, the advantage of helium imaging compared to other imaging modalities in clinical applications will be further explored.

Keywords: Helium, Proton, Computed Tomography, Radiography, Particle Imaging, Stopping Power, Resolution.

https://doi.org/10.1515/cdbme-2017-0084

1 Introduction

Proton radiography (pRAD) and proton computed tomography (pCT), first proposed by Cormack [1], recently gained more interest, as treatment planning systems for particle radiotherapy require precise knowledge of the stopping power within the patient. So far, this quantity is obtained through a conversion from x-ray CT Hounsfield units, introducing large uncertainties. It has been shown, that proton imaging can reduce these uncertainties by measuring the stopping power tomographically [2] or by combining pRad and x-ray CT [3]. However, although proton imaging is advantageous over x-ray CT in various points, multiple Coulomb scattering (MCS) reduces the achievable spatial resolution and conventional x-ray CT reconstruction algorithms produce blurred images when applied to pCT.

To overcome the problem of MCS, various path estimation algorithms have been proposed for protons, of which the most likely path (MLP) algorithm is the most widely used [4-8]. Compared to protons, heavier ions suffer less from MCS, due to on average smaller deflection angles per scattering. Recently, a strict Bayesian framework to predict the most likely path for any ion has been presented

***Corresponding author: Lennart Volz:** German Cancer Research Center (DKFZ), INF280, 69120 Heidelberg, Germany, e-mail: l.volz@dkfz-heidelberg.de; Department of Physics and Astronomy, Heidelberg University, Heidelberg, Germany
Charles-Antoine Collins-Fekete: Départment de physique, de génie physique et d'optique et centre de recherche sur le cancer, Université Laval, Québec, Canada; Départment de radio-oncologie et CRCHU de Québec, CHU de Québec, Canada
Pierluigi Piersimoni: German Cancer Research Center (DKFZ), Heidelberg, Germany
Robert P. Johnson: SCIPP, University of California Santa Cruz, Santa Cruz, USA
Vladimir Bashkirov, Reinhard Schulte: Division of biomedical engineering sciences, department of basic sciences, Loma Linda University, Loma Linda, USA
Joao Seco: German Cancer Research Center (DKFZ), Heidelberg, Germany; Department of Physics and Astronomy, Heidelberg University, Heidelberg, Germany

and its precision depending on the ion species was investigated [9]. Results pointed towards helium ions to potentially yield the best spatial resolution while depositing less physical dose to the patient, than heavier ions.

To allow for the computation of the proposed path estimation algorithms, sophisticated detector systems are needed to measure the required information. Currently, pCT detector systems rely on fast silicon trackers, acquiring the particles initial and final position and direction, as well as an energy detector measuring the particles' residual energy.

As of now, no experimental study on helium ion imaging making use of the most recent path estimation algorithms has been conducted. In order to investigate the hypothesized benefits of helium ions in imaging, the prototype proton CT detector system developed by the U.S. pCT collaboration [10] was tested with helium beams at the Heidelberg Ion-Beam Therapy Centre (HIT).

2 Materials and methods

2.1 The most likely path algorithm

Path reconstruction algorithms are crucial for accurate particle imaging, as they reduce the uncertainty introduced by MCS. Path estimation algorithms usually require the initial and final position (x) and direction (p) of the particles. The most widely used path reconstruction algorithm, the MLP, is a probabilistic method to estimate the particles lateral displacement and angular deflection at certain depth [4][11]. Schulte *et al.* [6] proposed a matrix based Bayesian MLP formalism, that derives the proton path solving the maximum likelihood problem based on Fermi-Eyges theory. Recently, Collins-Fekete *et al.* [9] revisited and extended the Bayesian approach to work for the estimation of heavier ions trajectories. Additionally, the complex, time-consuming MLP algorithm was linked to the recent, more efficient phenomenological approach [8]. The algorithm uses cubic splines and includes the information of the Water Equivalent Path Length (WEPL) and the Water Equivalent Thickness (WET) to derive an accurate path estimate. In this work, radiographies were reconstructed based on the phenomenological approach by Collins-Fekete *et al.* [12] employing the phenomenological cubic spline path algorithm. Tomographic images were reconstructed using a diagonally relaxed orthogonal projection (DROP) iterative algorithm enhanced by interleaved superiorization of the total variation (TV) of the reconstructed image (TVS) based on the MLP algorithm to yield accurate RSP values [13].

2.2 Phase 2 particle CT detector

In this study, a prototype particle detector system originally developed for proton beams by a collaboration of Loma Linda University (LLU), University of California Santa Cruz (UCSC) and California State University San Bernardino (CSUSB), namely the U.S. pCT collaboration, was used. The system is capable of detecting single event proton path information up to a rate of ~1MHz. The setup is shown in shown in **Figure 1**.

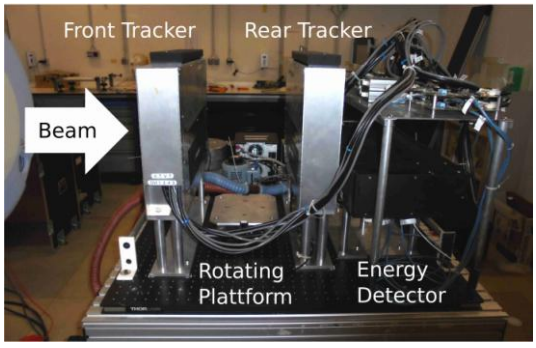

Figure 1: Prototype particle CT detector system first developed by the U.S. pCT collaboration. The system consists of two tracking detector systems, precisely measuring position and direction information, and an energy detector measuring the particles' residual energy.

The system comprises two tracking detectors (one preceding and one following the object to be imaged) consisting of silicon strip detectors (SSD). The silicon strips small pitch (0.228 mm) allows for high precision measurements with final sub-millimeter RMS resolution of 0.066 mm [14]. Stacking of silicon strips layers in alternate directions allows for 2-D measurement of the position. An energy/range detector measures the WEPL of the material through which the particle has passed in traversing the object. The energy detector has an aperture of 8.8 x 35.0 cm^2 and consists of five plastic (UPS-932A) scintillator stages (5.1 cm thick each) read out by photomultiplier tubes, resulting in a final energy resolution of 1% [14]. Prior calibration using a well-defined Polystyrene (RSP=1.03) wedge phantom is performed [15]. A rotating platform allows for fast CT scans and the detector is equipped with a high-speed data-acquisition system based on 14 FPGAs.

2.3 Experimental setup

Experiments were performed at the Heidelberg Ion-Beam Therapy Centre (HIT). The initial energy for helium was set to E_{He}=200.38 MeV/u and for protons E_p=200.11 MeV/u, where the small difference results from the accelerators

properties. A field of 10x20 cm^2 was irradiated using a raster scanning method with 10.2 mm FWHM per irradiation point for helium and 12.8 mm for protons. Particle rate was set to roughly 1 MHz to avoid events pile up in the energy calorimeter. For radiography ~10^7 histories were recorded, for tomography, 90 projections consisting of 2.5–4x10^6 histories each were acquired.

Radiographies were acquired of a phantom consisting of a 5.1 cm thick block of Polystyrene in front of a 4 cm thick Epoxy cylinder for evaluation of the spatial resolution using a sharp edge gradient technique. To investigate the stopping power accuracy and spatial resolution of HeCT and pCT, tomographies were acquired for the Catphan® (The Phantom Laboratory, Salem, New York, USA) high resolution module (CTP528) and sensitometry module (CTP404). For a case closer to the clinical reality, a CIRS paediatric head model HN715 (CIRS, Norfolk, Virginia, USA) was assessed and finally, a custom-built phantom was investigated, comprising an animal tissue sample (pig leg) enclosed in a 2% Agarose mixture.

3 Results

The radiographies spatial resolution was investigated using a sharp edge gradient technique. pRad yields a $MTF_{10\%}$=3.35 lp/cm, whereas for HeRad a $MTF_{10\%}$=6.07 lp/cm is observed.

HeCT of the Catphan® high resolution and sensitometry modules are shown in **Figure 2**. The images were reconstructed with slice thickness of 1.25mm and 512x512 pixels per slice. Using the Catphan high resolution module, the spatial resolution of HeCT was assessed. Visually, up to 5 lp/cm can be resolved for HeCT. Relative stopping power (RSP) accuracy was investigated using the CTP404 sensitometry module and compared to theoretical values obtained from the composition data[15]. For each of the sensitometry modules inserts, the RSP accuracy is 2.5% relative error or better. The reconstructed HeCT images yield visible ring and streak artefacts.

For a more complex scenario, the CIRS paediatric head model HN715 was investigated tomographically (see **Figure 3A)**. The tomography was reconstructed, with 256x256 pixels per slice and 1.25 mm slice thickness. The images allow for a clear differentiation between bone and soft tissue, as well as air cavities.

For a scenario closer to clinical reality, a custom-built animal tissue phantom is investigated (see **Figure 3B)**. A cut through Tibia and Fibula is visible, as well as the surrounding muscle/fat areas and the skin. The images yield good contrast between bone and soft tissue, but low contrast when it comes to soft tissue and the 2% Agarose mixture.

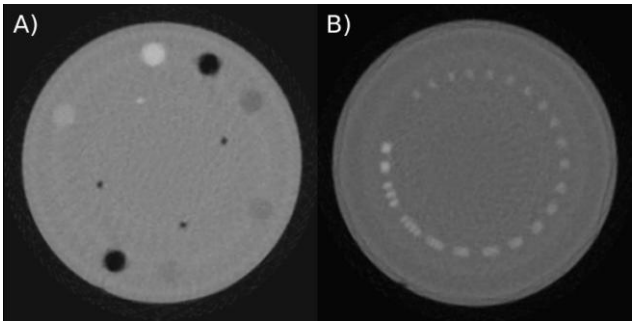

Figure 2: HeCT of A) the Catphan® CTP404 sensitometry module and B) the CTP528 high resolution module reconstructed using the DROP-TVS reconstruction algorithm with 512x512 pixel per slice and slice thickness of 1.25 mm. The phantom was scanned from 90 projections consisting of ~2.5x10^6 particles each.

4 Discussion

HeRad and HeCT were investigated at HIT using a prototype particle CT detector. The system proved to work well for the use of helium beams, but ring artefacts are present in the reconstructed HeCT images. This might be due to uncertainties in the calibration of the energy detector for helium ions, as the calibration method was originally developed for the use with protons and is still subject to further optimization.

The hypothesized increase in spatial resolution could be verified for radiographies using the pCT detector system ($MTF_{10\%}$=3.35 lp/cm for protons and $MTF_{10\%}$=6.07 lp/cm for helium ions). For tomographies, a low number of 90 projections was taken, effectively limiting the spatial resolution and resulting in streak artefacts stemming from under sampling of the system matrix. Nevertheless, the images yielded good contrast properties and allow for quantitative investigation of the stopping power accuracy.

The relative stopping power (RSP) values were computed for every insert of the CTP404 sensitometry module and compared to theoretical values from composition data [15]. The RSP accuracy was better than 2.5% for every insert and is subject to further optimization. As of now, the stopping power accuracy seems to be lower, than achievable with proton beams [15]. This could be due to processes involved in helium imaging that are not yet taken into account in the detector calibration. Further theoretical and practical investigation of the RSP accuracy of proton and helium imaging is needed.

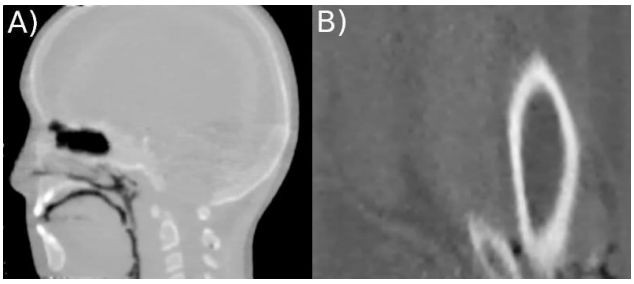

Figure 3: Vertical slice of a HeCT of A) the CIRS pediatric head phantom model HN715 (CIRS, Norfolk, Virginia, USA) and B) the custom build animal tissue phantom reconstructed using the DROP-TVS iterative reconstruction algorithm with 256x256 pixel per slice and slice thickness of 1.25 mm. The phantom was scanned using 90 projections consisting of ~4x10^6 particles each.

A helium tomography of the CIRS paediatric head phantom model HN715 was presented as a more complex scenario closer to clinical reality. The images yield a good contrast in between bone and soft tissue. In addition to the aforementioned artefacts, streak artefacts appeared in the presence of air cavities. Since the MLP prediction shows a higher RMS deviation in air cavities, these artefacts might be a result of the reconstruction algorithm and could be overcome by employing an improved path estimation algorithm.

The observed low contrast in between the animal tissue sample and the surrounding medium for the custom-built tissue phantom is expected, since the used Agarose mixture has a similar RSP value to soft tissue. Despite the artefacts, fatty areas are distinguishable from regular muscle tissue and the images yield good bone and soft tissue contrast.

5 Conclusion

In this study, computed tomographies with helium ion beams are presented and helium radiographies were investigated using a prototype detector system allowing for the use of the latest path reconstruction algorithms. Helium radiography proved to yield better spatial resolution than achievable with proton beams. For helium tomographies the spatial resolution was limited, probably because of the low number of projections taken. Future studies will focus on building a detector system further optimized for the use of helium ion beams. Eventually helium ion imaging will be compared to other available imaging modalities.

Author's Statement

Research funding: This work is supported by the German Cancer Research Centre (DKFZ). Conflict of interest: Authors state no conflict of interest. Informed consent: Informed consent is not applicable. Ethical approval: The conducted research is not related to either human or animals use.

References

[1] Cormack A.M. Representation of a Function by Its Line Integrals, with Some Radiological Applications. J. App. Phys. 1963; 43:2722–2727.
[2] Zygmanski P. The measurement of proton stopping power using proton-cone-beam computed tomography. Phys. Med. Biol. 2000; 45:511.
[3] Collins-Fekete C.-A. et al. A new optimization method for pre-treatment patient specific stopping power by combining proton radiography and x-ray CT. Med. Phys. 2016; 43:5756–3757
[4] Williams D.C. The most likely path of an energetic charged particle through a uniform medium. Phys. Med. Biol. 2004;49:2899.
[5] Li T., et al. Reconstruction for proton computed tomography by tracing proton trajectories: A Monte Carlo study. Med. Phys. 2006; 33:699.
[6] Schulte R.W. et al. A maximum likelihood proton path formalism for application in proton computed tomography. Med. Phys. 2008; 35:4849–4856
[7] Erdelyi B. A comprehensive study of the most likely path formalism for proton-computed-tomography. Med. Phys. 2009; 54:6095–6122
[8] Collins-Fekete C.-A. et al. Developing a phenomenological model of the proton trajectory within a heterogeneous medium required for proton imaging. Phys. Med. Biol. 2015; 60:5071–5082
[9] Collins-Fekete C.-A. et al. A theoretical framework to predict the most likely ion path in particle imaging. Phys. Med. Biol. 2017; 62:1777
[10] Schulte R. et al. Overview over the llumc/ucsc(csusb phase 2 proton CT project. Trans. Am. Nucl. Soc 2012; 106:59–62
[11] Schneider U, Pedroni E. Multiple coulomb scattering and spatial resolution in proton radiography. Med. Phys. 1994; 21:1657–1663
[12] Collins-Fekete C.-A. et al. A maximum likelihood method for high resolution proton radiography/proton CT. Phys. Med. Biol. 2016; 61:8232
[13] Penfold S. et al.Total variation superiorization schemes in proton computed tomography image reconstruction. Med. Phys. 2010:5887–5895
[14] Johnson R. et al. A fast experimental scanner for proton CT: Technical performance and first experience with phantom scans. IEEE Trans. Nucl. Sci. 2015; 63:52–60
[15] Piersimoni et al. The effect of beam purity and scanner complexity on proton CT accuracy. Med. Phys. 2017; 44:284–298